Oxide thin-film electronics on carbon fiber reinforced polymer composite

Article (Accepted Version)

Oxide Thin-film Electronics on Carbon Fiber Reinforced Polymer Composite

Niko Münzenrieder, *Member, IEEE,* Júlio Costa, Giuseppe Cantarella, Christian Vogt, *Student Member, IEEE,* Luisa Petti *Member, IEEE,* Alwin Daus, Stefan Knobelspies, and Gerhard Tröster, *Senior Member, IEEE*

***Abstract*—In this letter, the direct fabrication of amorphous Indium-Gallium-Zinc-Oxide thin-film transistors (TFTs) and circuits on a commercial carbon fiber reinforced polymer (CFRP) substrate is demonstrated. The CFRP is encapsulated with a ≈10.6 µm thick resin layer, although the surface roughness and temperature sensitivity of the substrate are not ideal for the fabrication of electronic devices, we present depletion mode TFTs exhibiting a field effect mobility of 18.3 $cm^2V^{-1}s^{-1}$, and a common source amplifier, providing a voltage gain of 8 dB and a −3 dB cutoff frequency of 11.5 kHz. The amplifier does not require any input bias voltage and can hence be directly used to condition signals originating from various transducers e.g. piezoelectric strain sensors used to monitor the structural integrity of CFRP elements. This opens the way to the fabrication of smart mechanical CFRP parts with integrated structural integrity monitoring systems.**

***Index Terms*—Thin-film transistors, carbon reinforced polymer, amorphous-IGZO, voltage amplifier.**

I. Introduction

TRADITIONALLY, electronic devices are fabricated on semiconductor wafers. Nevertheless, a variety of other substrates, mostly used for the fabrication of thin-film devices, became more important in the last years. Examples are paper, for cheap and biodegradable applications [1], [2], glass panels for large area electronics [3], and plastic foils for flexible or roll-to-roll fabricated electronics [4], [5]. Another motivation for the use of unconventional substrates is the aim to unobtrusively integrate electronic functionality into common items such as textiles [6]. This calls for electronic devices on substrates with similar mechanical properties as everyday objects. Since most of the involved materials are temperature sensitive, new semiconductor materials, in particular amorphous Indium-Gallium-Zinc-Oxide (IGZO) [7], became more important due to their ability to combine low temperature processability and good electrical performance. At the same time, these materials exhibit better electrical performance than organic semiconductors or amorphous silicon [5]. A class of materials which recently attracted a lot of attention in the mechanical engineering community are carbon fiber reinforced polymers (CFRPs). These materials combine a high tensile strength and low weight [8] which make them an integral part of many modern mechanical systems such as bridges, wind turbine blades, car frames, or airplane wings [9]. However, maintenance of such components is expensive and labor intensive [10]. The direct fabrication of electronic components such as sensors and the associated conditioning circuits on CFRP would enable the realization of mechanical parts with integrated strain or fatigue monitoring systems.

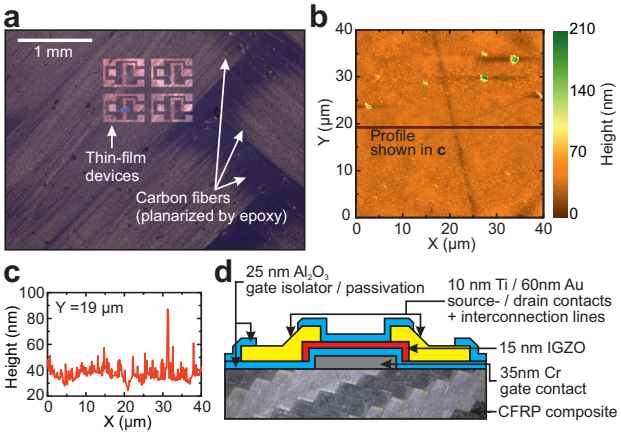

Fig. 1. a) Micrograph of oxide thin-film devices directly fabricated on a commercial carbon fiber reinforced polymer plate (encapsulated with a ≈10.6 µm thick resin layer). b) Representative 2D surface structure and (c) surface profile of the CFRP substrate measured using an AFM. d) Schematic cross-section of the TFTs.

Here, we present to the very best of our knowledge, the first depletion mode TFTs and analog circuits directly fabricated on a commercial CFRP substrate. Although fabricated on a substrate not designed or optimized for the fabrication of semiconductor devices, the TFTs exhibit an average field effect mobility of 18.3 $cm^2V^{-1}s^{-1}$, while a common source amplifier, with power consumption as low as 130 µW, provides a voltage gain up to 8 dB without the need for DC input bias.

II. Materials and Device Fabrication

Thin-film devices (shown in Fig. 1a) were directly fabricated on CFRP substrates using standard thin-film deposition techniques and UV lithography.

A. Substrate

Commercial 5 mm thick carbon fiber reinforced polymer plates served as substrate. The CFRP is made from multiple layers of woven carbon fiber fabric embedded into a transparent epoxy resin. To prepare the substrate, 7.5 cm×7.5 cm

Manuscript received ....

N. Münzenrieder, and J. Costa are with the Sensor Technology Research Centre, University of Sussex Falmer, Brighton, BN19QT, UK (corresponding email: n.s.munzenrieder@sussex.ac.uk). N. Münzenrieder, G. Cantarella, C. Vogt, L. Petti, A. Daus, S. Knobelspies, and G. Tröster are with the Institute for Electronics at the Swiss Federal Institute of Technology Zürich, Zürich, 8092, Switzerland.

large samples were cut using a circular saw, and the CFRP was cleaned in acetone and IPA (this had no observable influence on the epoxy). Although the carbon fibers are highly conductive, the epoxy resin acts as insulating spacing layer and enables the fabrication of devices without additional substrate encapsulation. Additionally, the resin also flattens the surface of the substrate and allows the fabrication of thin-film devices. To quantify the surface properties, an AFM scan of the CFRP and a representative surface profile are shown in Fig. 1b and Fig. 1c, respectively. On the one hand side, a RMS surface roughness of 9.5 nm was measured. This value is only slightly worse than the surface roughnesses obtained from conventional polymer substrates such as polyimide foil (RMS =4.1 nm) [11]. At the same time, ≈20 nm deep scratches, and up to multiple hundreds of nanometer tall peaks are measured as well. Since the total thin-film device thickness is only around 100 nm these anomalies in the surface structure have to be considered during the device fabrication. Due to the woven structure of the carbon reinforcement, the thickness of the epoxy encapsulation is not constant. To shield the TFT channels (in particular within circuits) from capacitive coupling to the conductive carbon fabric, we used a bottom gate layout. The specific capacitance of the epoxy encapsulation was measured using (0.19 mm^2) Cr metal pads deposited on the substrate (where the bottom contact with the carbon fibers was achieved by mechanically removing the epoxy encapsulation in a small area in the substrate center). The thickness variation of the epoxy led to a specific capacitance varying between 288 pF/cm^2 and 387 pF/cm^2 (average value is 327 pF/cm^2). This confirms that compared to the capacitance of the gate insulator (280 nF/cm^2), only negligible capacitive coupling between the devices and the substrate can be expected. Assuming a room temperature ϵ_r of 3.9 for the epoxy [12], the average thickness of the resin is calculated to be 10.6 µm.

B. Thin-film devices and circuits

The schematic cross sectional structure, including materials and layer thicknesses, of the fabricated back channel passivated inverted staggered bottom gate TFTs is given in Fig. 1d. First, the substrate was treated with an ozone plasma to promote the adhesion of the following layers. 35 nm thick evaporated Cr was deposited on the CFRP and structured into gate contacts using wet etching. The gate was electrically insulated by 25 nm atomic layer deposited (ALD) Al_2O_3. The ALD deposition is performed at 150°C, which is the highest temperature found during the fabrication process. Although this temperature is lower than the decomposition temperature of the epoxy resin, it is larger than its glass transition temperature [13]. Hence, we observed a slight softening of the hot CFRP when handling the substrate after ALD, but no permanent deformation or change of the mechanical properties. Additionally, we didn't observe any effects of the temporary change of the substrate properties on any of the deposited layers. At the same time, the pinhole free and conformal ALD Al_2O_3 is essential for the gate insulator fabrication on the uneven CFRP substrate. Room temperature RF magnetron sputtering was used to deposit 15 nm of amorphous IGZO

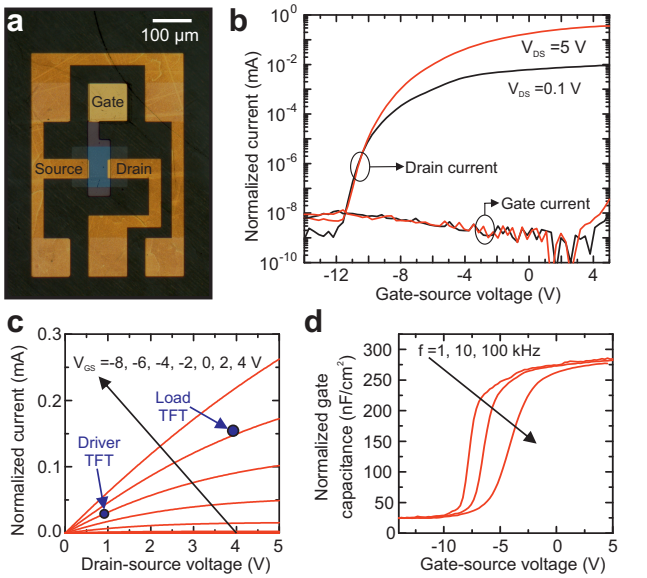

Fig. 2. a) Micrograph of a single IGZO TFT. Corresponding transfer (b), output (c) and capacitance-voltage (d) characteristics normalized by the channel width and length [c) also shows the bias points of the TFTs within the designed circuit]

from a ceramic IGZO target with a composition of In:Ga:Zn =1:1:1 mol. The IGZO and Al_2O_3 layers were structured by two independent wet etching steps. To form source and drain contacts as well as circuit interconnection lines, 10 nm of Ti (as adhesion layer) and 60 nm of Au were evaporated and structured by lift-off. Afterwards ALD deposition and structuring of a second Al_2O_3layer (25 nm), as device passivation, finalized the fabrication process.

III. Results and Discussion

TFT current-voltage and capacitance-voltage characterization under ambient conditions was performed with a Keysight B1500A parameter analyzer. Performance parameters were extracted using standard MOSFET equations [14]. AC characterization of circuits was performed using a Agilent 33220A function generator and a Tektronix MD03014 Oscilloscope with an input impedance of 1 MΩ and 13 pF.

A. Transistors

A fully processed TFT with a W/L ratio of 1 (50 µm/50 µm) can be seen in Fig. 2a. The low surface quality of the substrate is reflected in the matt appearance of the metallic gold pads, and the only moderate yield of ≈40 %. Nevertheless it has to be mentioned that the yield for TFTs with channel length >50 µm is above 90 %. The representative full DC characterization of the TFT, including I_D-V_{GS}, I_D-V_{DS}, and C_G-V_{GS} measurements are shown in Fig. 2b, c, and d, respectively. The TFT exhibits a threshold voltage V_{TH} of −7.9 V and an average field effect mobility of 18.3 $cm^2V^{-1}s^{-1}$ (the values for the Hall mobility are typically similar to the field effect mobility on these TFTs). Compared to similar TFTs on polyimide, featuring a slightly positive V_{TH} [5], the TFTs on CFRP exhibit a significantly more negative V_{TH}.

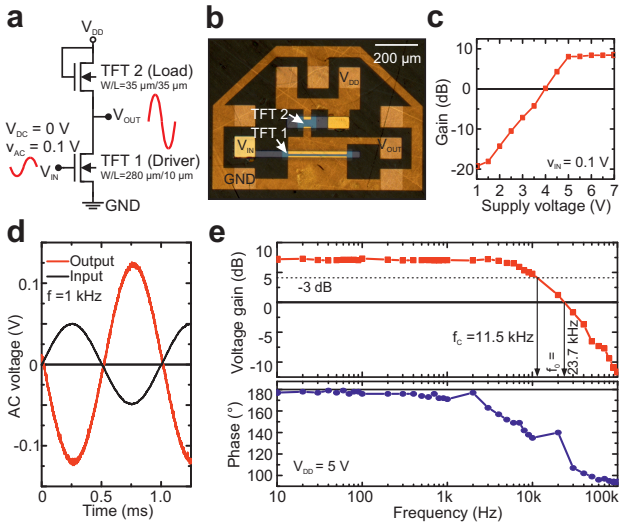

Fig. 3. a) Circuit schematic of a common source amplifier with active load showing the W/L ratios of the TFTs, as well as the input AC and DC voltages. b) Micrograph of the fabricated amplifier on CFRP substrate. c) Variation of the overall voltage gain with supply voltage. d) Representative sinusoidal input and output signals and e) Bode plot of the amplifier.

This is due to the high outgasing rates of epoxy resin under vacuum conditions [15], emitting H_2O and Nitrogen [16], and the associated unintentional doping of the IGZO during the sputter deposition. Both species are known to decrease the threshold voltage of IGZO TFTs [17], [18]. As very negative voltages (-12 V) were applied, a clockwise hysteresis was observed due to significant gate bias stress (480 MV/m). The average V_{TH} shift is 420 mV. For high V_{GS} values the field effect mobility reduces to 10.7 $cm^2V^{-1}s^{-1}$, consequently the maximum transconductance g_m only reaches a values of 49 $\mu S_\square$. Since the contact resistance is not dominant for this long channel TFT (see also the output characteristic in Fig. 2c), the reduction of mobility is attributed to an increased interface scattering of the charge carriers [5]. The interface quality is also responsible for the subthreshold swing (inverse of subthreshold slope) of 396 mV/dec . Due to the high quality ALD deposited gate insulator, the gate leakage current always stays below 0.1 nA, and the on-off current ratio is as high as 7×10^7. The gate capacitance measurement reflects the geometry of the channel and source drain to gate overlaps. Furthermore, the overlap and channel capacitance in the on and off regime do not depend on the frequency or sweep direction. At the same time, and similarly to the transfer characteristic, a small (<500 mV) clockwise hysteresis was observed in the subthreshold range. The frequency dependency in the substhreshold range was previously observed for TFTs with identical layer structure, and is caused by trap states [11]. We expect that the TFT performance could be further improved by employing a thick substrate encapsulation and planarization layer.

B. Analog circuits

Based on the TFT measurements a fully integrated common-source amplifier was designed and fabricated. Fig. 3a and 3b show the circuit schematic and micrograph. Due to the use of depletion mode TFTs no DC bias is needed at the input (bias points are illustrated in Fig. 2c). The estimated maximum transit frequency of the driver TFT (based on g_m and C_G) is 7.3 MHz [19]. First the optimal supply voltage of the circuit was evaluated by measuring its voltage gain for different V_{DD} (Fig. 3c). It can be seen that the voltage gain reaches unity at a V_{DD} of 4.1 V and saturates at voltages above 5 V (this result is nearly independent of the input voltage amplitude). Hence V_{DD} =5 V was used for the following characterization. Here the amplifier has a current consumption of 26 µA, and the DC voltage offset of the inverted output signal is 0.9 V. A representative pair of input and output signals is shown in Fig. 3d. The output signal exhibits no visible distortion, and a low frequency voltage gain of 8 dB. The frequency performance of the circuit is summarized by the Bode plot shown in Fig. 3e. The graph can be used to extract a −3 dB cutoff frequency of 11.5 kHz and a unity gain frequency of 23.7 kHz (limited by the current driving capabilities of the TFTs in the circuit). These performance parameters make the presented circuit compatible with the sampling rate of most sensor applications.

IV. Conclusion

We presented, to the best of our knowledge, the first analog amplifier circuits directly fabricated on a light weight and highly robust CFRP substrate. Low temperature fabrication processes and IGZO semiconductor were used to fabricate depletion mode TFTs with a threshold voltage of −7.9 V and an average field effect mobility of 18.3 $cm^2V^{-1}s^{-1}$ on the commercial composite substrate exhibiting a RMS surface roughness of 9.5 nm. Integrated common source amplifiers with an active load element provide a gain of 8 dB and a gain bandwidth product of 59.5 kHz (unity gain frequency times low frequency gain). These amplifiers not only demonstrate the reliability of the proposed technology, but can also be used as sensor readout circuit and hence open a route towards smart mechanical CFRP parts with integrated front-end conditioned sensor systems.

Acknowledgment

The authors would like to thank Matthew Large and Alan Dalton for their support on AFM measurements.

References

[1] Y. H. Jung, T.-H. Chang, H. Zhang, C. Yao, Q. Zheng, V. W. Yang, H. Mi, M. Kim, S. J. Cho, D.-W. Park *et al.*, "High-performance green flexible electronics based on biodegradable cellulose nanofibril paper," *Nature communications*, vol. 6, 2015. http://dx.doi.org/10.1038/ncomms8170

[2] D. Tobjörk and R. Österbacka, "Paper electronics," *Advanced Materials*, vol. 23, no. 17, pp. 1935–1961, 2011. http://dx.doi.org/10.1002/adma.201004692

[3] K. Hayashi, Y. Kato, and M. Kunigita, "Effect of glass substrate characteristics on pattern tolerance in inverted staggered type tft array fabrication," in *SID Symposium Digest of Technical Papers*, vol. 46, no. 1. Wiley Online Library, 2015, pp. 1372–1374. http://dx.doi.org/10.1002/sdtp.10129

[4] R. F. Service, "Patterning electronics on the cheap," *Science*, vol. 278, no. 5337, pp. 383–384, 1997. http://dx.doi.org/10.1126/science.278.5337.383

[5] L. Petti, N. Münzenrieder, C. Vogt, H. Faber, L. Büthe, G. Cantarella, F. Bottacchi, T. D. Anthopoulos, and G. Tröster, "Metal oxide semiconductor thin-film transistors for flexible electronics," *Applied Physics Reviews*, vol. 3, no. 2, p. 021303, 2016. http://dx.doi.org/10.1063/1.4953034

[6] A. Nathan, A. Ahnood, M. T. Cole, S. Lee, Y. Suzuki, P. Hiralal, F. Bonaccorso, T. Hasan, L. Garcia-Gancedo, A. Dyadyusha *et al.*, "Flexible electronics: The next ubiquitous platform," *Proc. of the IEEE*, vol. 100, no. 13, pp. 1486–1517, 2012. http://dx.doi.org/10.1109/JPROC.2012.2190168

[7] K. Nomura, H. Ohta, A. Takagi, T. Kamiya, M. Hirano, and H. Hosono, "Room-temperature fabrication of transparent flexible thin-film transistors using amorphous oxide semiconductors," *Nature*, vol. 432, no. 7016, pp. 488–492, 2004. http://dx.doi.org/10.1038/nature03090

[8] R. Selzer and K. Friedrich, "Mechanical properties and failure behaviour of carbon fibre-reinforced polymer composites under the influence of moisture," *Composites Part A: Applied Science and Manufacturing*, vol. 28, no. 6, pp. 595–604, 1997.

[9] D. Gay, *Composite materials: design and applications*. CRC press, 2014.

[10] A. Baltopoulos, N. Polydorides, L. Pambaguian, A. Vavouliotis, and V. Kostopoulos, "Damage identification in carbon fiber reinforced polymer plates using electrical resistance tomography mapping," *Journal of Composite Materials*, vol. 47, no. 26, pp. 3285–3301, 2013. http://dx.doi.org/10.1177/0021998312464079

[11] N. Münzenrieder, L. Petti, C. Zysset, T. Kinkeldei, G. A. Salvatore, and G. Tröster, "Flexible self-aligned amorphous InGaZnO thin- film transistors with sub-micrometer channel length and a transit frequency of 135 MHz," *IEEE Trans. on El. Dev.*, vol. 60, no. 9, pp. 2815–2820, 2013. http://dx.doi.org/10.1109/TED.2013.2274575

[12] T. Furukawa, K. Fujino, and E. Fukada, "Electromechanical properties in the composites of epoxy resin and pzt ceramics," *Japanese Journal of Applied Physics*, vol. 15, no. 11, p. 2119, 1976. http://iopscience.iop.org/1347-4065/15/11/2119

[13] K. Zhang, Y. Gu, Z. Zhang *et al.*, "Effect of rapid curing process on the properties of carbon fiber/epoxy composite fabricated using vacuum assisted resin infusion molding," *Materials & Design*, vol. 54, pp. 624–631, 2014. http://dx.doi.org/10.1016/j.matdes.2013.08.065

[14] S. Sze and K. Ng, *Physics of Semiconductor Devices*. John Wiley and Sons, 2007.

[15] A. Gupta, K. K. Smt, J. Santhanam, and P. Vijendran, "Outgassing from epoxy resins and methods for its reduction," *Vacuum*, vol. 27, no. 2, pp. 61–63, 1977. https://doi.org/10.1016/S0042-207X(77)80764-1

[16] R. Brown, "Outgassing of epoxy resins in vacumm," *Vacuum*, vol. 17, no. 9, pp. 505–509, 1967. https://doi.org/10.1016/0042-207X(67)90175-3

[17] P.-T. Liu, Y.-T. Chou, L.-F. Teng, F.-H. Li, and H.-P. Shieh, "Nitrogenated amorphous ingazno thin film transistor," *Applied Physics Letters*, vol. 98, no. 5, p. 052102, 2011. http://dx.doi.org/10.1063/1.3551537

[18] H. S. Shin, Y. S. Rim, Y.-G. Mo, C. G. Choi, and H. J. Kim, "Effects of high-pressure h2o-annealing on amorphous igzo thin-film transistors," *physica status solidi (a)*, vol. 208, no. 9, pp. 2231–2234, 2011. http://dx.doi.org/10.1002/pssa.201127243

[19] N. Münzenrieder, G. A. Salvatore, L. Petti, C. Zysset, L. Büthe, C. Vogt, G. Cantarella, and G. Tröster, "Contact resistance and overlapping capacitance in flexible sub-micron long oxide thin-film transistors for above 100 mhz operation," *Applied Physics Letters*, vol. 105, no. 26, p. 263504, 2014. http://dx.doi.org/10.1063/1.4905015